ELSEVIER

Biochimica et Biophysica Acta 1468 (2000) 41–54

BIOCHIMICA ET BIOPHYSICA ACTA

BBA

www.elsevier.com/locate/bba

Estimations of lipid bilayer geometry in fluid lamellar phases

S.C. Costigan [a,b,1], P.J. Booth [a,1], R.H. Templer [b,*]

[a] *Department of Biochemistry, Imperial College, London SW7 2AY, UK*

[b] *Department of Chemistry, Imperial College, London SW7 2AY, UK*

Received 1 November 1999; received in revised form 3 April 2000; accepted 13 April 2000

Abstract

The excess water bilayer thickness, $d_{l,0}$, and molecular area, A_0, of lipid amphiphiles in the fluid lamellar phases of dioleoylphosphatidylcholine (DOPC) and dipalmitoleoylphosphatidylcholine (DPolPC) have been estimated between 15 and 50°C and for dimyristoylphosphatidylcholine (DMPC) between 25 and 50°C. These determinations have been made from X-ray measurements on samples of known water composition. With respect to temperature, T, $d_{l,0}$ and A_0 are well fitted to a linear equation. We find $d_{l,0}$ (Å) = $(35.68 \pm 0.02) - (0.0333 \pm 0.0006)T$ (°C) and A_0 (Å^2) = $(70.97 \pm 0.05) + (0.136 \pm 0.001)T$ (°C) for DOPC, $d_{l,0}$ (Å) = $(35.2 \pm 0.1) - (0.068 \pm 0.003)T$ (°C) and A_0 (Å^2) = $(59.7 \pm 0.2) + (0.210 \pm 0.006)T$ (°C) for DMPC, and $d_{l,0}$ (Å) = $(34.54 \pm 0.03) - (0.0531 \pm 0.0009)T$ (°C) and A_0 (Å^2) = $(67.12 \pm 0.09) + (0.173 \pm 0.003)T$ (°C) for DPolPC. The accuracy of these estimates depends largely on how accurately the excess water point is determined. Ideally, reliable X-ray and compositional data will be available around the excess water and it may be found by simple inspection, but this is the exception rather than the rule, since samples close to water excess normally sequester sizeable amounts of water in defects, which lead to an underestimate of $d_{l,0}$. and overestimate of A_0. In this paper, we report a methodology for identifying and removing such data points and fitting the remaining data in order to determine the excess water point.

Keywords: X-ray diffraction; Phosphocholine; Bilayer thickness; Methodology

1. Introduction

An essential element in the study of model membranes and their interactions with bilayer proteins and other amphipathic molecules, is the precise and accurate determination of the structural parameters of the fluid bilayer. Specifically, the average area per lipid and the average thickness of the lipid bilayer are of importance. For example, the lipid molecular geometry determined experimentally is an input in computer simulations of the behaviour of membrane proteins [1], the lipid bilayer thickness is important when accounting for hydrophobic mismatch between membrane protein and membrane [2–5] and the molecular area is a critical variable in calculating the free energy of protein insertion into the membrane [6]. The contents of this paper arose from our own need to obtain values of bilayer thickness in our studies of the refolding kinetics of bacteriorhodopsin as a function of lipid bilayer composition [7–9].

Unfortunately, determinations of the lipid area and length in the fluid membrane have varied quite

* Corresponding author. Fax: +44-171-594-5801; E-mail: r.templer@ic.ac.uk

[1] Present address: Department of Biochemistry, Bristol University, Bristol BS8 1TD, UK.

0005-2736/00/$ – see front matter
PII: S0005-2736(00)00220-0

significantly. For example, for dipalmitoylphosphatidylcholine (DPPC), lipid area values have been reported between 57.6 and 71.7 Å^2 ([10] and references therein), for DMPC values reported vary from 59.5 to 65.7 Å^2 [11–15], and for DOPC the range spans 70–82 Å^2 [13,15–18]. Part of this variability may be due to differences in the methods used to determine the molecular geometry. Two methods are currently in use to obtain this type of information, both of which aim to determine the molecular area and length of the lipid in the fluid lamellar or L_α phase. It is assumed that under excess water conditions, the molecular geometry in this condensed phase is the same as that of the molecule in a unilamellar vesicle.

In the first approach, the bilayer electron density profile may be calculated directly from X-ray diffraction spectra. This is in principle the best and most direct method, but unfortunately liquid crystals in the L_α phase only give low resolution X-ray spectra. Therefore, certain assumptions about the structure of the bilayer and the water/lipid interface have to be made to allow data interpretation. To circumvent the low resolution problem, one variation has been introduced in which one characterises a lipid in the gel phase, where better resolution spectra are obtained, and subsequently calculates structural differences between the L_α and the gel phase by comparing the peak to peak distances of spectra from gel and L_α phase lipids [19]. Comparisons between lipids have even been made this way [16].

In this paper, we will be concerned with the alternative method introduced by Luzzati and Husson [20]. Here lipid geometry in the L_α phase is determined from a knowledge of the exact amount of water needed to fully hydrate a lipid (the excess water point), the unit cell repeat spacing of the phase and the density of the lipid and water. The unit cell spacing, or lattice parameter, of the L_α phase is determined by X-ray diffraction as a function of the water composition. We call the resulting plot the swelling curve. The repeat spacing increases with water content, until it reaches the water excess point whereupon it reaches the equilibrium value, which allows one to determine both the excess water point and the equilibrium lattice parameter. In Luzzati and Husson's method, it is then assumed that the lipid and water pack into well-defined, separate layers [18,20], Fig. 1. With a knowledge of the molecular volume of the lipid and water, the bilayer thickness can then be calculated.

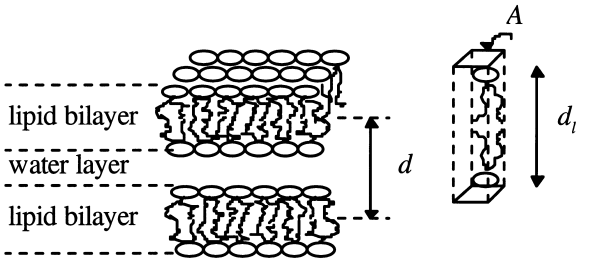

Fig. 1. The model of the fluid lamellar phase, which assumes that the water and lipid bilayers are completely separate. d, the unit cell spacing; A, the average cross-sectional area per lipid; and d_l, lipid bilayer thickness.

In principle, this is fine, but in practice it is rather difficult to determine the excess water point precisely, because the data tend to be noisy. To get around this, it is normal practice to fit the swelling curve and determine the water composition at which the fit to the swelling data is equal to the excess water lattice parameter.

The generally accepted drawback of this method is that sample preparations at molar water to lipid ratios of approximately 20 and higher, have been shown to induce multi-lamellar vesicles (MLVs) and water pockets [21,22]. This means that water is being sequestered in defects and grain boundaries, but the model assumes that it lies between regularly spaced bilayers. This leads to an overestimation of the water contribution to the unit cell spacing and hence the calculations of lipid length are systematically underestimated and those of area are systematically overestimated. Others [11,18] have attempted to overcome this systematic error by using only data obtained at lower water contents and extrapolating to excess water conditions. The extrapolation is calculated from the measured, lateral, isothermal compressibility of the lipid bilayer, an approach that has the merit that it uses a physical model of the swelling to fit the data. However, in this paper, we present evidence that just at the point that MLVs and water pockets begin to form, an additional, repulsive interbilayer force becomes significant, which the extrapolation does not take into account. This repulsive force means that in fact additional water, beyond that determined by the compressibility extrapolation, is taken up by the phase. If this is the case, the result

of such extrapolation is an overestimation of the bilayer thickness and an underestimation of the lipid area.

The occurrence of MLVs and the accompanying water pockets is known to be influenced by the sample preparation method (see e.g. [21,23]), and their influence on the derivation of the lipid structural parameters has not been quantified. In this study, a new method is presented, relying on the temperature dependence of the swelling, to discern between samples where excess water is available due to bilayer defects and where the sample has truly reached excess water conditions.

When this is done, one is, however, left with at least one other difficulty. How is the swelling curve to be fitted without any a priori theoretical form for the swelling? In this paper, we have taken a heuristic approach, by observing that the variation in bilayer thickness with molar ratio of water to lipid is apparently quadratic, and then using this form to fit the swelling curve.

2. Materials and methods

2.1. Sample preparation

1,2-Dioleoyl-*sn*-glycero-3-phosphatidylcholine (DOPC), 1,2-dimyristoyl-*sn*-glycero-3-phosphatidylcholine (DMPC) and 1,2-dipalmitoleoyl-*sn*-glycero-3-phosphatidylcholine (DPolPC) were obtained from Avanti Polar Lipids (Alabaster, AL, USA). Their purity was given as $>99\%$. Thin-layer chromatography, carried out using 65 parts chloroform, 25 parts methanol and 4 parts distilled water as eluting agents and iodine vapour as the locating agent, produced one spot for DOPC and DMPC. For DPolPC a small second spot was seen in some of the plates. The high R_f value would suggest it might be triglycerides [24]. Given its apparent low level of occurrence, no further purification was performed, but this finding might be related to the slightly higher variation found in the DPolPC data versus the DMPC and DOPC data. Lipids were stored at -20°C under nitrogen and freeze-dried from cyclohexane before use.

Samples were prepared according to an approach reported previously [23]. X-ray capillaries (1.5 mm diameter; W. Müller, Berlin) were weighed on a Sartorius microbalance (± 1 μg precision) before and after addition of lipid and water. Lipid was solubilised in cyclohexane (sometimes small amounts of methanol were added) and distributed between the pre-weighed capillaries such that the total amount of lipid per capillary was approximately 10–50 mg. The lipid was lyophilised in the capillary for at least 4 h, but usually overnight. Different amounts of water were then added, and the capillaries sealed with heat shrink tubing (RS Components, Northants, UK). The heatshrink was removed immediately after an experiment and the capillary weighed to establish the final water content. Triply distilled and deionised water was used for hydrating the samples. The capillaries were left to equilibrate overnight or longer at room temperature, in the dark. X-ray diffraction was recorded from three different locations along the capillary's length. If the repeat spacing differed by 1 Å or more, the capillary was centrifuged up and down once. If this process needed to be repeated more than two times, the sample was discarded on the assumption that too many defects in the lamellar structure would be induced by this much mechanical mixing. Except for the equilibration time at room temperature, all samples were stored at 4°C until examination.

In calculating the molar ratio of water to lipid, n_w, where

$$n_w = \frac{\text{mol water}}{\text{mol lipid}} \quad (1)$$

we assume that even after freeze drying, there remain two water molecules per lipid.

2.2. X-ray measurements

X-ray diffraction was used to establish the unit cell spacing, d, of the L_α phase. A rotating anode X-ray generator (GX-20, Nonius, Netherlands) was used, equipped with Franks double-mirror X-ray optics producing a point focus. The detection system consists of an image intensified X-ray detector coupled to a CCD detector [25]. The precision of an individual X-ray diffraction measurement of the lattice parameter was ± 0.3 Å. Temperature control of the samples was achieved by means of Peltier devices, to a precision of ± 0.03°C. During temperature

scans, the sample was left at each temperature for at least 5 min before each exposure. Longer equilibration times applied to a few samples indicated no significant change was measured after this time. Scans were taken at 5°C intervals from 15 to 50°C.

2.3. Density measurements

Lipid densities were measured with a Paar DMA 60 Density Meter and DMA 602 Density Measuring Cell from Paar Scientific (Graz, Austria). The density meter was calibrated with water and air. Sample temperature was controlled to within ±0.02°C, which gave rise to an uncertainty of 6×10^{-6} g cm^{-3} in the measured density. Great care was taken to ensure there were no air bubbles in the samples (water was degassed before use, water contents were kept slightly above water excess point to keep viscosity manageable and samples were visually inspected at regularly intervals during the measurements). Our measurements, Fig. 2, are in agreement with the available literature values for DMPC and DOPC [16,26,27].

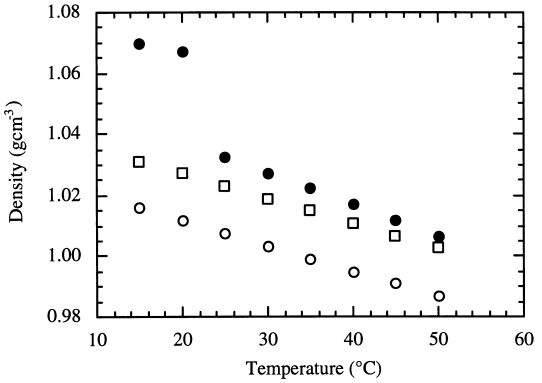

Fig. 2. Measured lipid densities of DOPC (open circles), DMPC (filled circles) and DPolPC (open squares). All values are averages of three separate measurements. The step change in density observed for DMPC occurs at the chain melting transition around 23–24°C. The molecular volumes in the fluid phase calculated from these data fitted well to a linear equation with respect to temperature. For DOPC, $v_l = (1268.2\pm0.1)+(1.092\pm0.004)T$; for DMPC, $v_l = (1061.5\pm0.2)+(1.133\pm0.0004)T$; and for DPolPC $v_l = (1161.0\pm0.1)+(0.956\pm0.003)T$.

2.4. Data analysis

The molecular geometry may be calculated within the model of the L_α phase shown in Fig. 1 from a knowledge of lipid and water volumes, v_l and v_w, the molar composition and the measured d spacing. The bilayer thickness, d_l, is given by

$$d_l = \frac{d}{\left(1 + n_w\frac{v_w}{v_l}\right)} \quad (2)$$

the molecular cross-sectional area, A, is given by

$$A = \frac{2v_l}{d_l} \quad (3)$$

and the water layer thickness between the bilayers, d_w, is given by

$$d_w = d - d_l. \quad (4)$$

In the study by Klose and co-workers [21], four distinct regions in the swelling curves of egg yolk lecithin in the L_α phase were structurally and morphologically defined using X-ray diffraction and freeze fracture electron microscopy. At low water contents, the unit cell spacing was found to increase at the slowest rate with respect to water composition. This was found to correspond to a morphology of large extended planar sheets of lipid bilayers and was found to extend up to 10 mol of water per lipid. It is believed that this region is where there is a tight association of the water molecules to the headgroup [14,22]. Once the tightly associated waters had been added, the swelling curve displayed a steeper and apparently linear increase in unit cell spacing with n_w. This region contained mainly large extended bilayers and the water was still homogeneously distributed between them, but defects in the bilayers began to appear. At greater water compositions, they observed a region, which we will call region III, where the increase of unit cell spacing with n_w was less pronounced and the freeze fracture preparations were characterised by the presence of vesicle-like structures and water droplets alongside the large extended sheets of bilayers. Beyond this, they found that excess water had been reached and the unit cell spacing remained constant with respect to water composition. In this region, MLVs with a wide distribution of size existed [21,22].

These observations indicate that there are at least two important elements in a reasonable analysis of the swelling curves of the L_α phase. The first is that we need to be able to identify samples in the compositional regime of region III and eliminate them from our determination of the excess water point. The drawback of the Luzzati method is that the occurrence of the sequestration of water in region III skews the bilayer thickness calculations to a lower value, and the calculated water thickness to a higher value [21,22]. The second is that we need to decide on a reasonable mathematical form for the variation of d with respect to n_w in order to fit the remainder of the data on the swelling curve and so determine the excess water composition by intersection with the excess water value of d.

In order to identify samples which are in region III, we have used the temperature-dependent behaviour of the L_α phase. Below the water excess point, it is well established that the bilayer thickness decreases and area per phospholipid increases with temperature [14,18,27–29]. Hence, for fixed n_w the increase in lipid area must be accompanied by a decrease in d_w and therefore an overall decrease of d with temperature. Mathematically this can be expressed as $(\partial d/\partial T)_{n_w}<0$. However, when the water supply is no longer limited this need not be the case. Indeed where there are fluctuation repulsions between bilayers we would expect water *uptake* with increasing temperature. In Fig. 3 the change of unit cell spacing with changing temperature, at fixed water content is plotted. As expected based on the above, at lower water contents the unit cell spacing decreases at a constant rate with increasing temperature for all three lipids, i.e. $(\partial d/\partial T)_{n_w}$ has a constant, negative value. As of approximately $n_w \approx 30$ the unit cell spacing's decrease with temperature lessens and at higher water contents even becomes an increase. This indicates that, despite the fixed water content of the sample, at higher temperatures, the bilayers are taking up extra water from somewhere. Either because the sample is in excess water conditions and extra water is freely available, or because significant amounts of sequestered water are available in local bilayer defects. The excess water points are easily identifiable because the unit cell spacing equals the constant water excess unit cell spacing found at the higher water contents. The remainder of the points, where $(\partial d/\partial T)_{n_w}$ is larger than the constant negative value observed at lower water contents, but the unit cell spacing has not yet reached the water excess value, are in region III. These data points are eliminated from our determination of the excess water point.

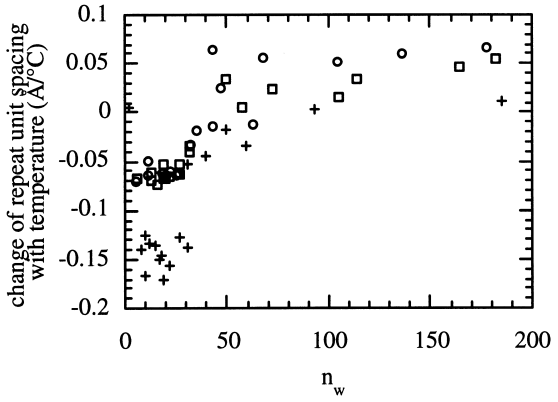

Fig. 3. The identification of samples in region III. The rate of change of unit cell spacing with respect to temperature at fixed water composition, $(\partial d/\partial T)_{n_w}$, is plotted against the water composition, n_w, for DPolPC (open circles) from 15–50°C, DOPC (open squares) from 15–50°C and DMPC (crosses) from 25–50°C. Where $(\partial d/\partial T)_{n_w}$ deviates from the constant negative values seen at low water compositions, the system is either in excess water, or in region III. Samples in region III are easily identified by the fact that the unit cell spacing is less than the excess water value.

Having eliminated these points from each of the isothermal swelling curves we then have to fit the remaining data. Previously, it was noted the swelling appeared linear, therefore data were fit to a linear line. However, a linear fit of d with respect to n_w implies that both d_l and A remain constant during the addition of water to the system. This is clearly not the case over a wide water content range, such as seen from our measurements of d_l as a function of water composition, Fig. 4, and noted earlier by different authors [14,21,22]. As a rule, empirical approaches should use the simplest function that will still represent the data. The next simplest model is a quadratic function:

$$d_l = d_{l,0} + \alpha(n_{w,0} - n_w)^2 \quad (5)$$

where $d_{l,0}$ and $n_{w,0}$ are the bilayer thickness and water composition in excess water, respectively, and α is a scaling coefficient for the quadratic. The choice of this form is entirely heuristic and reflects the phys-

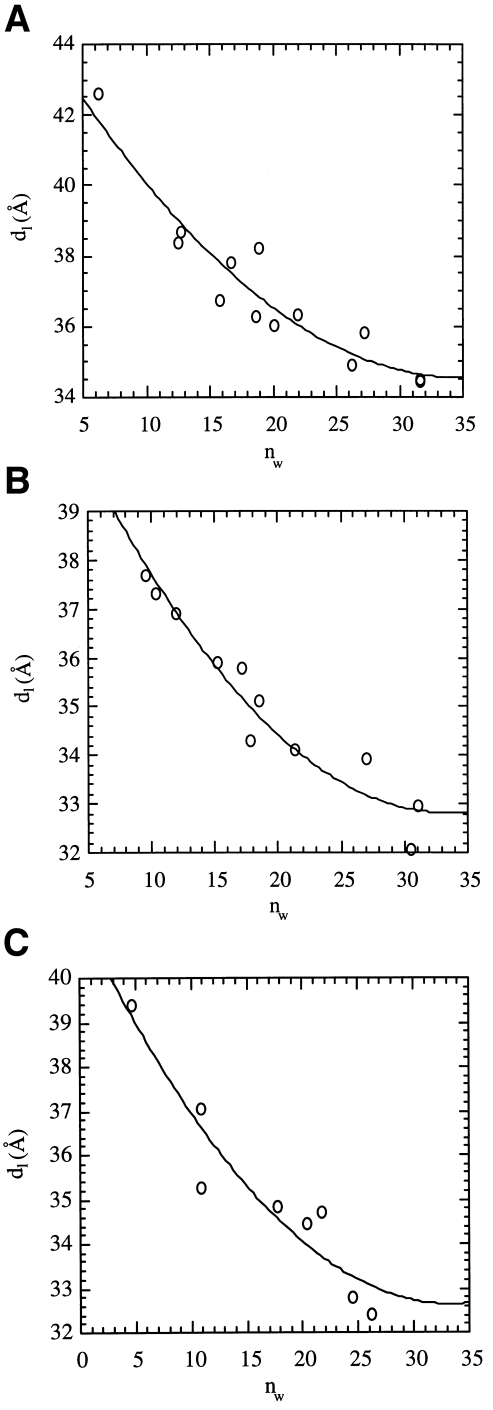

Fig. 4. The variation in bilayer thickness, d_l, with respect to water composition, n_w. Representative data recorded at 35°C for (A) DOPC, (B) DMPC and (C) DPolPC has been fitted using Eq. 5. The bilayer thickness is determined via equation Eq. 2 and data from region III and excess water have been excluded.

ical intuition that as one adds water to the fluid lamellar phase the bilayer thickness should not reach a stationary value at the excess water equilibrium abruptly, but smoothly. The quadratic form is also consistent with the observations recorded by Klose and co-workers [21], in as far as the cross-sectional area of the lipids does expand rapidly initially and the final stages of the swelling of the unit cell will be nearly linear, so long as α is not too great.

From Eqs. 2 and 5 and noting that d_l is set by the excess water value of the lattice parameter, d_0, we have the heuristic function with which we fit the swelling curve

$$d = \left[\frac{d_0}{(1 + n_{w,0}\ v_w/v_l)} + \alpha\ (n_{w,0} - n_w)^2\right][1 + n_w\ v_w/v_l] \tag{6}$$

From the fit, we obtain $n_{w,0}$ and α and we can then find $d_{l,0}$ by fitting our data of $d_l(n_w)$ using Eq. 5. The excess water area per molecule, A_o, is then given by substituting $d_{l,0}$ into Eq. 3.

3. Results

As an example of the swelling curves for each lipid, we show plots of the data taken at 35°C and the fit to these data, Fig. 5. Similar data have been obtained at the other temperatures; that is between 15 and 50°C for DOPC and DPolPC, but only between 25 and 50°C for DMPC, since at lower temperatures, DMPC is in the gel phase [30]. In the case of DMPC and DPolPC, samples were found that were evidently in region III [21], i.e. a sample morphology with long lifetime metastable defects sequestering water. The data points are shown in the figures and begin to appear around $n_w \approx 30$. Data presented in Koenig et al. [11] on DMPC and stereoyl-oleoyl-phosphocholine demonstrate deviations of the Luzatti derived area per lipid values compared to the NMR data around $n_w \approx 20$. Furthermore, bilayer defects observed by electron microscopy appeared around the same water composition [21,22]. The apparent slightly later onset of region III in this study implies that the concentration of MLVs and water pockets, is at first probably too low to measurably affect the unit cell spacing at this point. However, given the

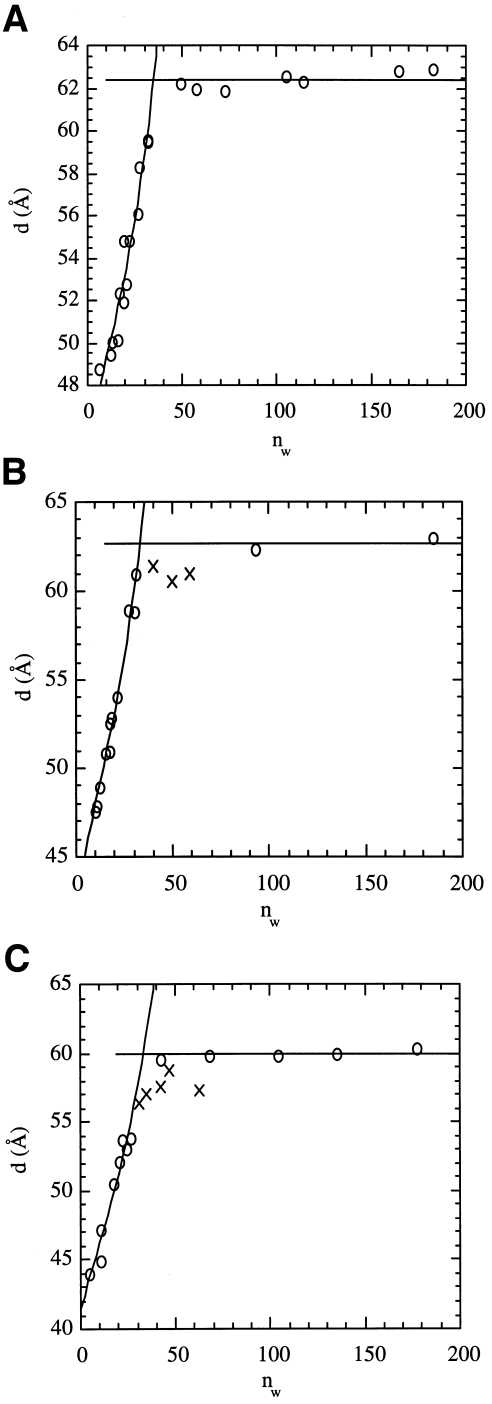

Fig. 5. Swelling curves at 35°C for (A) DOPC, (B) DMPC and (C) DPolPC. The horizontal line is the mean value of the excess water lattice parameter, d_0, and the intersecting curve is the fit to the swelling data using Eq. 6. Data points identified as belonging to region III and therefore excluded from the fit are represented by ×. Data points beyond $n_w = 200$ are not shown, although they have been used in determining d_0.

sensitivity to sample preparation [21,23], caution must be exercised in cross study comparisons.

Nevertheless, we did test to see if we could obtain any evidence of water sequestered in defect pockets in our DOPC samples, even though none had been detected by our measurements of $(\partial d/\partial T)_{n_w}$. To do this, we measured the lattice parameter of three samples below the excess water point before and after shear alignment between concentric X-ray capillaries. Since sample alignment should reduce the defect density in a lamellar phase, we reasoned that any defects not detected by our measurement of $(\partial d/\partial T)_{n_w}$, might be revealed by a systematic increase in lattice parameter after shear. The alignment after shear was evidenced by the powder rings sharpening into arcs. However, there was no measurable systematic difference between the aligned and powder samples. We measured samples at several points along the length of the X-ray capillary, but found no evidence of a systematic increase, to within the random variation in d of approximately ± 0.4 Å. Similarly, after 50 heating and cooling cycles between 15 and 50°C on unaligned samples of DOPC, we found no change in d spacing.

Examples of plots of bilayer thickness as a function of water composition and the accompanying fits used to obtain $d_{l,0}$ are shown in Fig. 4. The nonlinearity of d_l with respect to n_w is particularly evident in the cases of DOPC and DMPC.

From these fits and the measured densities, the lipid areas in excess water can also be calculated. Tables 1–3 list the values for the average molecular geometry as well as the limiting hydration and excess water lattice parameter as a function of temperature for DOPC, DMPC and DPolPC, respectively. We have plotted the variation in $d_{l,0}$, $d_{w,0}$ (the water layer width at excess), $n_{w,0}$, and A_0, with temperature in Fig. 6. In each case, over the temperature span that we have studied, it appears that the variation is linear, the fitted form being recorded in Table 4. In addition, we have provided linear relationships for the molecular volumes as a function of the temperature, calculated from the measured densities.

In agreement with expectations [14,18,28], $d_{l,0}$ decreases as a function of the temperature, whilst, at the same time, A_0 increases with the temperature. Within experimental error, the excess water bilayer

Table 1
Measured molecular geometry and hydrational behaviour of DOPC in the L_α phase

T (°C)	v_w (Å^3)	v_l (Å^3)	d_0 (Å)	$d_{l,0}$ (Å)	$n_{w,0}$	A_0 (Å^3)
15	29.946	1284.7	61.88 ± 0.12	35.17 ± 0.20	32.65 ± 0.80	73.06 ± 0.42
20	29.974	1290.0	62.01 ± 0.15	35.02 ± 0.19	33.21 ± 0.78	73.67 ± 0.40
25	30.008	1295.4	62.12 ± 0.15	34.86 ± 0.19	33.76 ± 0.77	74.32 ± 0.40
30	30.049	1300.8	62.26 ± 0.17	34.67 ± 0.20	34.46 ± 0.83	75.04 ± 0.43
35	30.096	1306.3	62.39 ± 0.15	34.54 ± 0.19	35.00 ± 0.82	75.64 ± 0.42
40	30.150	1311.8	62.61 ± 0.24	34.33 ± 0.19	35.83 ± 0.86	76.42 ± 0.42
45	30.212	1317.3	62.77 ± 0.25	34.16 ± 0.20	36.51 ± 0.93	77.12 ± 0.45
50	30.279	1322.9	62.92 ± 0.28	34.03 ± 0.20	37.07 ± 0.98	77.75 ± 0.46

thickness of DMPC and DPolPC are the same in the L_α phase. This does not seem unreasonable, given that although DPolPC is two CH_2 groups longer than DMPC, it contains a *cis* double bond. The DOPC bilayer is thicker by approximately 2 Å than DPolPC and DMPC. This difference would be rather small if the molecular cross-sectional area of DOPC and DPolPC were the same. From Fig. 6D it can be seen that the measurements indicate that DOPC is approximately 3 Å^2 greater in cross-section than DPolPC. Again, this is not unreasonable since we would expect the longer unsaturated chain to exert a greater lateral pressure at a fixed cross-sectional area. This picture is consistent with the 9-Å^2 reduction in cross-sectional area of the saturated C_{14} chain of DMPC compared to DOPC. Furthermore, the fit to the area expansion as a function of temperature for DMPC, Table 4, can be used to determine the thermal area expansivity (defined as $1/A_0 \times (\partial A_0/\partial T)$). At 29°C, we find a value of $(3.2 \pm 0.1) \times 10^{-3}$ °C^{-1} which is in reasonable agreement with the value determined on a study of giant DMPC vesicles at 29°C, where a value of $(6.8 \pm 1.0) \times 10^{-3}$ °C^{-1} has been reported [31].

The temperature-dependent increase in the interbilayer spacing $d_{w,0}$ is consistent with fluctuational repulsions between the bilayers [18,32,33]. It is also in agreement with the hypothesis that the change in $(\partial d/\partial T)_{n_w}$ from a constant negative to a positive value as large pools of water appear in the system, is due to fluctuation repulsions drawing water into the space between bilayers. Recent studies into the vapour paradox in bilayers have also confirmed the importance of bilayer undulations in reaching full hydration in the L_α phase [34,35]. By increasing the opportunity for undulations, water saturated, oriented bilayers were shown to further increase their unit cell spacing by several Ångstroms [36]. For example, in the case of dilauroylphosphatidylcholine, the interbilayer distance has been shown to be approximately 5 Å larger in the presence of undulatory fluctuation forces than when these were suppressed by immobilisation of the bilayers on a mica surface [18]. From our measurements on DMPC, we find a 5.0 ± 0.1-Å increase in $d_{w,0}$ when the system goes into the L_α phase from the gel phase (data not shown). Making the assumption that this difference is entirely due to fluctuation repulsions present [18,32,37], the agreement with the previous estimate is good. Indications of a temperature-dependent, bilayer repulsion not accounted for by hydration force theories has been suggested before for DMPC [38]. In this

Table 2
Measured molecular geometry and hydrational behaviour of DMPC in the L_α phase

T (°C)	v_w (Å^3)	v_l (Å^3)	d_0 (Å)	$d_{l,0}$ (Å)	$n_{w,0}$	A_0 (Å^3)
25	30.008	1089.9	62.87 ± 0.19	33.60 ± 0.18	31.74 ± 0.69	64.88 ± 0.35
30	30.049	1095.5	62.58 ± 0.25	33.18 ± 0.15	32.37 ± 0.59	66.03 ± 0.31
35	30.096	1101.1	62.73 ± 0.21	32.82 ± 0.14	33.38 ± 0.62	67.10 ± 0.29
40	30.150	1106.8	62.63 ± 0.26	32.55 ± 0.14	33.95 ± 0.63	68.01 ± 0.29
45	30.212	1112.5	63.11 ± 0.50	32.28 ± 0.13	35.18 ± 0.67	68.93 ± 0.28
50	30.279	1118.3	62.99 ± 0.13	31.82 ± 0.16	36.03 ± 0.81	70.29 ± 0.35

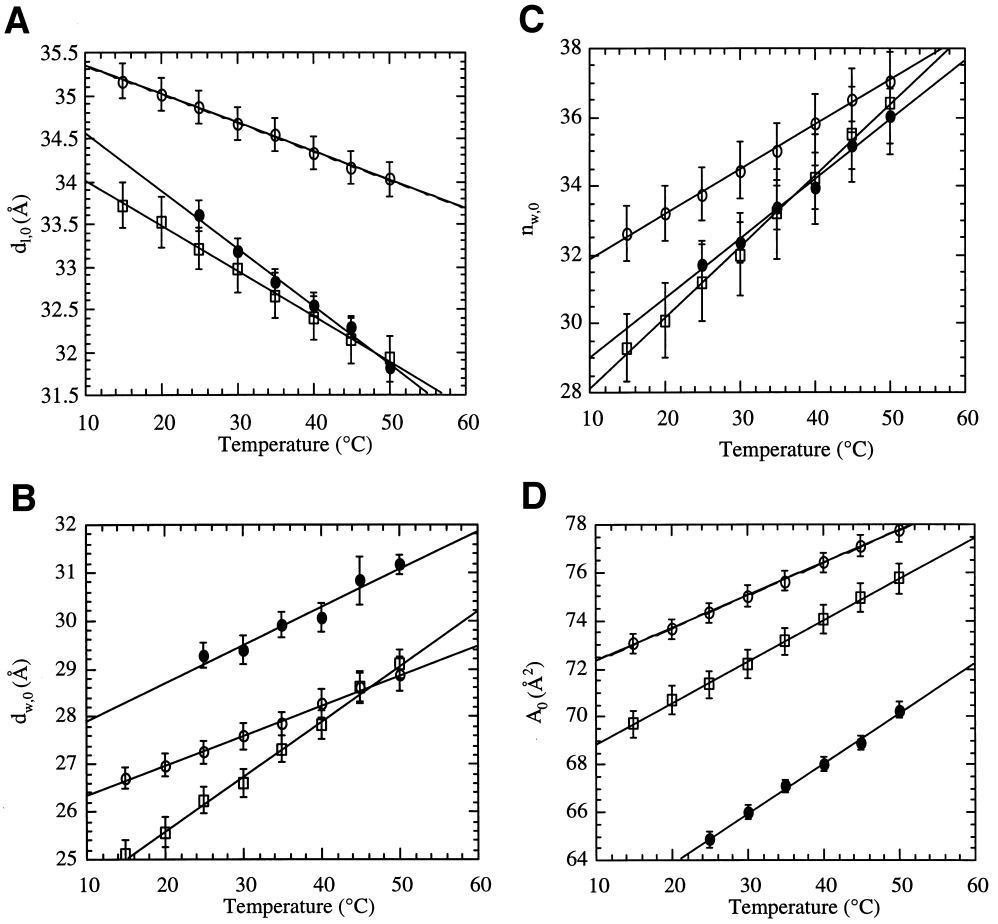

Fig. 6. The temperature-dependent behaviour of DOPC (open circles), DMPC (filled circles) and DPolPC (open squares) in excess water. (A) The variation in excess water bilayer thickness, $d_{l,0}$ with temperature. (B) The variation in water layer thickness, $d_{w,0}$, at the excess point as a function of temperature. (C) The variation in excess water composition point, $n_{w,0}$, with temperature. (D) The variation in molecular cross-sectional area, A_0, with temperature in excess water.

work, this repulsion is apparently stronger for DMPC than for DOPC and DPolPC. This is also consistent with a fluctuational repulsion, since the magnitude of the repulsive force is inversely proportional to the bilayer bending rigidity [33] and we would anticipate that the bending rigidity of the saturated lipid would be less than that of the unsaturated species.

Table 3
Measured molecular geometry and hydrational behaviour of DPolPC in the L_α phase

T (°C)	v_w (Å^3)	v_l (Å^3)	d_0 (Å)	$d_{l,0}$ (Å)	$n_{w,0}$	A_0 (Å^3)
15	29.946	1175.5	58.836 ± 0.094	33.72 ± 0.27	29.3 ± 1.0	69.72 ± 0.56
20	29.974	1180.1	59.097 ± 0.091	33.52 ± 0.29	30.1 ± 1.1	70.41 ± 0.61
25	30.008	1184.8	59.455 ± 0.097	33.21 ± 0.25	31.2 ± 1.1	71.35 ± 0.54
30	30.049	1189.6	59.57 ± 0.13	32.96 ± 0.27	32.0 ± 1.2	72.18 ± 0.60
35	30.096	1194.3	59.979 ± 0.088	32.66 ± 0.26	33.2 ± 1.3	73.14 ± 0.58
40	30.150	1199.2	60.21 ± 0.15	32.39 ± 0.26	34.2 ± 1.3	74.05 ± 0.59
45	30.212	1204.0	60.75 ± 0.12	32.13 ± 0.26	35.5 ± 1.4	74.95 ± 0.61
50	30.279	1208.9	61.02 ± 0.14	31.92 ± 0.26	36.4 ± 1.5	75.75 ± 0.62

4. Discussion

4.1. Fitting the swelling curve

The choice of a quadratic form for $d_l(n_w)$ is largely heuristic and discussed in more detail in Section 2.4. Looking at the experimental data of $d_l(n_w)$ in Fig. 4, it might seem that a simpler form would be linear

$$d_l = \beta n_w + (d_{l,0} - \beta n_{w,0}) \quad (7)$$

where β is the gradient and all other terms are as previously defined. However, this form has the unphysical behaviour that the shrinking of the bilayer width with added water to the L_α phase, stops abruptly as we reach the excess water point. For argument's sake, we go on to see what happens when we use Eq. 7 to derive the form of $d(n_w)$,

$$d = \left[\beta(n_w - n_{w,0}) + \frac{d_0}{(1 + n_{w,0}\ v_w/v_l)}\right](1 + n_w\ v_w/v_l) \quad (8)$$

and then fit some swelling data with this form and compare it to the fit from equation Eq. 6, Fig. 7. In the data of Fig. 7, the reduced χ^2 for the fit from Eq. 6 is 1.1, but rises to 1.9 for the fit to Eq. 8. The reason for the poorer fit to Eq. 8 lies in the fact that this form is incapable of modelling the initially slow increase in d with water composition. This problem recurs for all the data we have collected. This has also been observed by many other authors [14,15,17,21,22,27]. Generally, the lower water content data points have then been left out from the linear fits leading to the water excess point. This sometimes meant there were only very few points to fit to.

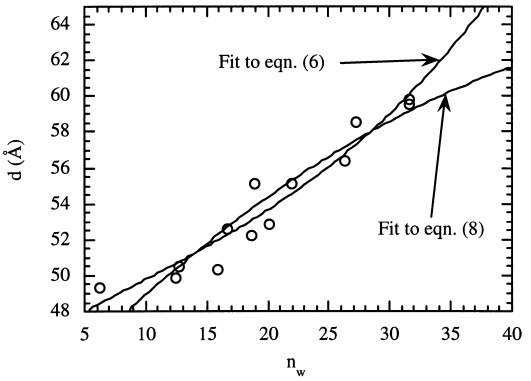

Fig. 7. Fitting the swelling curve for DOPC at 35°C. Fitting the swelling curve under the assumption that bilayer thickness shrinks linearly with water composition (Eq. 8) gives a poorer fit than the assumption that the bilayer thickness shrinks quadratically (Eq. 6).

Besides the empirical observation that a non-linear equation better allows us to fit the data over a large water content range, qualitative, theoretical considerations of the forces governing bilayer separation also point to a non-linear relation. The first few water molecules added to lipid bilayers interact strongly with the lipid headgroups [22] and are located partially between the headgroups [40], therewith releasing some of the intrabilayer pressure from steric and electrostatic repulsions between neighbouring headgroups [18]. Thus, at very low water contents, the water molecules contribute only partially to an increase in bilayer separation. As the intra-bilayer repulsion decreases with added water, the repulsive bilayer 'hydration' forces will grow in importance and extra added water molecules will tend to contribute more and more to increasing the

Table 4
The parameters for linear fits to the experimentally determined molecular geometry and hydration in the the L_α phase as a function of the temperature, T

	DOPC		DMPC		DPolPC	
	a_0	a_1	a_0	a_1	a_0	a_1
v_l (Å^3)	1268.2 ± 0.1	1.0919 ± 0.003	1061.4 ± 0.1	1.135 ± 0.004	1161.0 ± 0.1	0.955 ± 0.004
$d_{l,0}$ (Å)	35.68 ± 0.02	−0.0333 ± 0.0006	35.2 ± 0.1	−0.068 ± 0.003	34.54 ± 0.03	−0.0531 ± 0.0009
$d_{w,0}$ (Å)	25.72 ± 0.06	0.063 ± 0.002	27.1 ± 0.3	0.080 ± 0.008	23.3 ± 0.1	0.116 ± 0.003
$n_{w,0}$	30.62 ± 0.09	0.129 ± 0.003	27.2 ± 0.3	0.174 ± 0.008	26.0 ± 0.2	0.207 ± 0.004
A_0 (Å^2)	70.97 ± 0.05	0.136 ± 0.001	59.7 ± 0.2	0.210 ± 0.006	67.12 ± 0.09	0.173 ± 0.003

The data have been fitted using the equation $y = a_0 + a_1 T$ where y is the appropriate variable in column one, divided by the units shown to make it dimensionless and T is in °C.

bilayer distance. As the water content and bilayer separation increases, the equilibrium of 'hydration', van der Waals and thermal bilayer fluctuation forces will be influenced less and less by the repulsive forces between headgroups within one monolayer, i.e. more and more the water molecules will contribute to increasing the bilayer separation. Only when all of each new water molecule contributes to the bilayer separation, will the separation become linearly proportional to the increase in water content.

4.2. Systematic errors in the evaluation of molecular geometry

There are at least two sources of significant systematic errors in our determinations of $n_{w,0}$, $d_{l,0}$ and A_0. Let us first consider the assumption that the freeze-dried phosphatidylcholines are in fact dihydrated. If one assumes that the lipid is entirely dehydrated after lyophilisation then one must subtract two waters per lipid from the measurements of n_w. After fitting the data, there is a decrease in the value of $n_{w,0}$ by approximately two waters per lipid and a decrease in the magnitude of α. However, the net effect on the determination of $d_{l,0}$ upon subsequently fitting the data of $d_l(n_w)$ is rather small. For example, at 35°C we find: $d_{l,0} = 34.4 \pm 0.2$ Å for dehydrated DOPC, whereas $d_{l,0} = 34.5 \pm 0.2$ Å if it is dihydrated; in the case of DMPC $d_{l,0} = 32.5 \pm 0.2$ Å if it is dehydrated and 32.8 ± 0.1 Å if it is dihydrated and for DPolPC we find 32.3 ± 0.3 Å if it is dehydrated and 32.7 ± 0.3 Å if it is dihydrated. In other words, in the context of the fitting form we have used and the quality of the data, any systematic error due to assuming that the lipids are dihydrate is at the level of our errors.

The second source of systematic error is one where we are not able to estimate the magnitude of its possible effect. This source of error is the observation that d_0 can vary between different observers by as much as 3 Å, e.g. for DOPC at 25°C d_0 has been reported between 61 and 64 Å [15,17], and even within single studies, variations as great as this have been reported, e.g. DPPC [40], and DOPC [17]. The source of these variations is not understood, but apparently widespread. Since the precision of our measurements is a few tenths of Ångtroms, it seems reasonable to assume that the accuracy of our measurements is at present limited by the variations in d_0 since they are an order of magnitude greater.

4.3. Fluctuation repulsion

As explained in the introduction, multi-lamellar vesicles (MLVs) and water pockets have been shown to occur at water contents close to the water excess point [21,22], leading to an overestimation of the water contribution to the unit cell spacing in the Luzatti method, and thus an underestimation of the lipid thickness. Because of this effect, researchers using Luzzati's method have attempted to find methods which get around this problem by extrapolating the swelling curve from the more reliable data at lower water compositions [18]. So far, this has been done by measuring the isothermal compressibility of the L_α phase at these low water compositions. This is done by applying an osmotic pressure to the phase to remove water between the bilayers and measuring the lattice parameter as a function of the applied osmotic pressure. Below $n_w \approx 20$, the forces between bilayers of zwitterionic amphiphiles are limited to van der Waals attraction and hydration repulsions. So the graph of lattice parameter as a function of applied osmotic pressure are fitted to the sum of these forces. To find $d_{l,0}$ the equilibrium between these opposing forces is found.

This extrapolation depends, of course, on their being no additional forces which make an appearance between $n_w \approx 20$ and excess. However, we would suggest that the data presented in this study indicates that at water contents closer to the water excess point, an additional bilayer repulsive force appears to start playing a role. A force that increases with increasing temperature, which suggests that the force is due to fluctuation repulsions. Thermal undulations are only of significance at higher water contents, since they require the conformational space between bilayers in order to propagate [18,32,33]. The fluctuations increase the repulsive pressure in the system which is not accounted for by current modelling. At the excess water point, we would therefore expect that there is in reality more water in the phase than the current calculations would indicate and hence the bilayer thickness calculated without taking account of fluctuation repulsions would be overestimated. As an aside, it is of interest

to note that quite a few studies have appeared recently investigating the 'anomalous swelling' of bilayers near the main transition. There is still controversy about the underlying causes of this swelling [41–45], but increased bilayer fluctuations have been implicated [41,43,44]. However, the effect investigated in those studies results in an increase of d_0 with decreasing temperature. The opposite effect is seen here (Tables 1–3). Mainly this apparent discrepancy is a result of the different temperature ranges under investigation. The 'anomalous swelling' only plays a role relatively near to the main transition point and is thus not expected to influence the DOPC and DPolPC measurements presented here. Based on reported data on DMPC [41,42,45], this effect might well be expected to influence our DMPC measurements at the lower temperatures. However, in our hands, no decrease of d_0 with increasing temperature at 25°C and above was found (Table 2). In general, it has been postulated that the 'anomalous swelling' is more noticeable for shorter chainlength lipids, but less so for DMPC and longer lipids [44]. The increase in bilayer fluctuations referred to in the 'anomalous swelling' phenomenon is postulated to be due to a reduction of the bending modulus of the membrane in the transition region [41]. The results presented here do not assume any changes in bending moduli and increases in the fluctuations are expected to be simply due to increases in temperatures increasing the entropy of the system. There is, indeed, some evidence to support the higher level of thermal undulations than formerly recognised, such as hypothesised in this work. In the case of DPPC, the range of osmotic pressures used in the analysis has been extended to include lower pressures than normally used, and calculated lipid areas have subsequently increased from 61.2 to 64.2 Å^2 [40]. This translates into a decrease in the estimated bilayer thickness of approximately 1 Å. When we compare our analyses to those of Rand and coworkers [18] on DOPC and DMPC, we observe the same pattern. For DOPC at 25°C we find $d_{l,0} = 34.8$ Å (using the linear equation for $d_{l,0}$ as a function of temperature), whereas using the isothermal compressibility extrapolation method, they find $d_{l,0} = 35.9$ Å. As we would predict our calculations give a narrower bilayer width, by 1 Å in this case. For DMPC, we find the same effect, our value being 33.4 Å, whereas the isothermal compressibility extrapolation estimates $d_{l,0} = 35.7$ Å; a 2 Å difference.

A related method for determining excess water molecular geometry uses NMR order parameter measurements of the water molecules interacting with the lipid headgroups. Translation of NMR order parameter data into absolute structural lipid parameters [11], uses lipid cross-sectional areas determined by X-ray diffraction at lower water concentrations to relate NMR-derived areas to absolute values. To obtain values at excess water compositions, one then extrapolates to these values using the change in area with water content, derived from the measurement of the order parameter. But unless a special protocol is used, only the change in area due to water that actually interacts with lipids directly is measured. This perhaps explains why it has been calculated by this technique that at 30°C, the excess water composition of DMPC is 22.2 mol of water per lipid [11]. We determine $n_{w,0}$ to be 32.4 at this temperature for DMPC. The extra water drawn in with bilayer fluctuations, is not expected to interact directly with the lipids, thereby complicating identification by NMR. Only recently has a protocol been developed where a distinction can be made between the waters present within multilamellar assemblies that do not interact directly with lipids, versus bulk waters [46,47]. With this method, the moles of interlamellar water per DOPC has been now been estimated to be 37.5 ± 1 at 30°C [48]. This compares favourably with our calculation of $n_{w,0} = 34.5$ and corresponds to a discrepancy of only 0.5 Å in $d_{l,0}$.

4. Conclusions

To the best of the authors' knowledge, no investigations of the temperature-dependent variation of the structural parameters of phosphatidylcholines at different hydrations have previously been published. Scanning in temperature and water composition apparently enables one to distinguish between samples that contain appreciable amounts of sequestered water below the excess water point, and those that do not. We have introduced a simple heurisitic swelling law to determine the molecular geometry of DOPC, DMPC and, for the first time, DPolPC in

the fluid lamellar bilayer. The data and the analysis we have presented strongly indicate that even with lipids which have a relatively high bending rigidity, the effects of bilayer fluctuation repulsions can be observed. The fluctuation repulsions only become apparent around molar ratios of water to lipid of approximately 30, the same composition at which we start to notice the fact that a sizeable fraction of the water is no longer stored between flat bilayers, but is sequestered in defects and grain boundaries between multi-lamellar vesicles. These two observations may be related. From a practical point of view, this means that if one wishes to take measurements of the isothermal compressibility of fluid bilayers at low water contents and then extrapolate these to equilibrium in order to determine the excess water bilayer thickness, the model must take into account the bilayer fluctuation repulsions. Since these repulsions become evident at exactly the point where water becomes sequestered in defects and grain boundaries, it is difficult to see exactly how this would be done.

Measurements of bilayer thickness have been made previously on both DOPC and DMPC [11–18,38–40]. In general, our results fall within the current range of values estimated for the bilayer thickness; our values are no more than 3 Å different from reported values. The values we have reported are neither systematically greater or less than those determined by these other groups. Within the measurements presented in the report, we find consistent patterns of behaviour. Increasing chainlength increases bilayer thickness and molecular cross-sectional area. The introduction of a *cis* double bond in the hydrocarbon chain increases the molecular cross sectional area and reduces the bilayer width. In this way, we find that DPolPC and DMPC have almost identical bilayer widths. This makes it likely that mixed DPolPC/DMPC vesicles will make a good vehicle for studying the effects of variations in lateral pressure on bilayer spanning proteins, since the addition of palmitoleic chains should lead to an increase in lateral pressure, but without a concomitant change in the bilayer's width.

Acknowledgements

We would like to thank J. Robins and A. Squires for their technical help. This work was made possible by Grant B08427 from the Biophysical and Biotechnology Science Research Council, as well as financial support from the Royal Society and the Rosenheim Research Fellowship awarded to P.J.B.

References

[1] P. Lagüe, M.J. Zuckermann, B. Roux, Protein inclusion in lipid membranes: a theory based on the hypernetted chain integral equation, Faraday Discuss. 111 (1998) 165–172.
[2] D.R. Fattal, A. Ben-Shaul, A molecular model for lipid–protein interaction in membranes: the role of hydrophobic mismatch, Biophys. J. 65 (1993) 1795–1809.
[3] T. Gil, J.H. Ipsen, O.G. Mouritsen, M.C. Sabra, M.M. Sperotto, M.J. Zuckermann, Theoretical analysis of protein organization in lipid membranes, Biochim. Biophys. Acta 1376 (1998) 245–266.
[4] N. Dan, S.A. Safran, Effect of lipid characteristics on the structure of transmembrane proteins, Biophys. J. 75 (1998) 1410–1414.
[5] T.P. Galbraith, B.A. Wallace, Phospholipid chain length alters the equilibrium between pore and channel forms of gramicidin, Faraday Discuss. 111 (1998) 159–164.
[6] G.S. Attard, W.S. Smith, A.N. Hunt, S. Jackowski, R.H. Templer, Modulation of CTP: phosphocholine cytidylyltransferase by membrane curvature elastic stress, Proc. Natl. Acad. Sci. USA (2000) in press.
[7] P.J. Booth, M.L. Riley, S.L. Flitsch, R.H. Templer, A. Farooq, A.R. Curran, N. Chadborn, P. Wright, Evidence that bilayer bending rigidity affects membrane protein folding, Biochemistry 36 (1997) 197–203.
[8] M.L. Riley, B.A. Wallace, S.L. Flitsch, P.J. Booth, Slow alpha helix formation during folding of a membrane protein, Biochemistry 36 (1997) 192–196.
[9] A.R. Curran, R.H. Templer, P.J. Booth, Modulation of folding and assembly of the membrane protein bacteriorhodopsin by intermolecular forces within the lipid bilayer, Biochemistry 38 (1999) 9328–9336.
[10] J.F. Nagle, Area/lipid of bilayers from NMR, Biophys. J. 64 (1993) 1476–1481.
[11] B.W. Koenig, H.H. Strey, K. Gawrisch, Membrane lateral compressibility determined by NMR and X-ray diffraction: effect of acyl chain polyunsaturation, Biophys. J. 73 (1997) 1954–1966.
[12] J.F. Nagle, R.T. Zhang, S. Tristram-Nagle, W.J. Sun, H.I. Petrache, R.M. Suter, X-ray structure determination of fully hydrated l(alpha) phase dipalmitoylphosphatidylcholine bilayers, Biophys. J. 70 (1996) 1419–1431.
[13] B.A. Lewis, D.M. Engelman, Lipid bilayer thickness varies linearly with acyl chain length in fluid phosphatidylcholine vesicles, J. Mol. Biol. 166 (1983) 211–217.
[14] M.J. Janiak, D.M. Small, G.G. Shipley, Temperature and compositional dependence of the structure of hydrated dimyristoyl lecithin, J. Biol. Chem. 254 (1979) 6068–6078.

[15] L.J. Lis, M. McAlister, N. Fuller, R.P. Rand, V.A. Parsegian, Interactions between neutral phospholipid bilayer membranes, Biophys. J. 37 (1982) 657–665.
[16] S. Tristram-Nagle, H.I. Petrache, J.F. Nagle, Structure and interactions of fully hydrated dioleoylphosphatidylcholine bilayers, Biophys. J. 75 (1998) 917–925.
[17] S.M. Gruner, M.W. Tate, G.L. Kirk, P.T.C. So, D.C. Turner, D.T. Keane, C.P.S. Tilcock, P.R. Cullis, X-ray-diffraction study of the polymorphic behavior of N-methylated dioleoylphosphatidylethanolamine, Biochemistry 27 (1988) 2853–2866.
[18] R.P. Rand, V.A. Parsegian, Hydration forces between phospholipid bilayers, Biochim. Biophys. Acta 988 (1989) 351–376.
[19] T.J. McIntosh, S.A. Simon, Area per molecule and distribution of water in fully hydrated dilauroylphosphatidylethanolamine bilayers, Biochemistry 25 (1986) 4948–4952.
[20] V. Luzzati, F. Husson, The structure of the liquid–crystalline phases of lipid–water systems, J. Cell Biol. 12 (1962) 207–219.
[21] G. Klose, B. König, H.W. Meyer, G. Schulze, G. Degovics, Small-angle X-ray-scattering and electron-microscopy of crude dispersions of swelling lipids and the influence of the morphology on the repeat distance, Chem. Phys. Lipids 47 (1988) 225–234.
[22] K. Gawrisch, W. Richter, A. Möps, P. Balgavy, K. Arnold, G. Klose, The influence of water concentration on the structure of egg yolk phospholipid/water dispersions, Stud. Biophys. 108 (1985) 5–16.
[23] S.C. Costigan, P.J. Booth, R.H. Templer, Swelling series and bilayer defects due to sample preparation, Mol. Cryst. Liq. Cryst. in press.
[24] K.-H. Gober, B.R. Günther, E.M. Lünebach, G. Repplinger, M. Wiedemann, in: G. Cevc (Ed.), Phospholipids Handbook, Dekker, New York, 1993, pp. 39–64.
[25] R.H. Templer, S.M. Gruner, E.F. Eikenberry, An image-intensified Ccd area X-ray-detector for use with synchrotron radiation, Adv. Electr. Electron Phys. 74 (1988) 275–283.
[26] J.F. Nagle, D.A. Wilkinson, Lecithin bilayers. Density measurements and molecular interactions, Biophys. J. 23 (1978) 159–175.
[27] Y. Kobayashi, K. Fukada, Characterization of swollen lamellar phase of dimyristoylphosphatidylcholine-gramacidin A mixed membranes by DSC, SAXS and densimetry, Biochim. Biophys. Acta 1371 (1998) 363–370.
[28] F.Y. Chen, W.C. Hung, Structural changes of lipid membrane induced by dehydration, Chin. J. Phys. 34 (1996) 1363–1372.
[29] A. Tardieu, V. Luzzati, F.C. Reman, Structure and polymorphism of the hydrocarbon chains of lipids. Lecithin–water phases, J. Mol. Biol. 75 (1973) 711–733.
[30] R. Koynova, M. Caffrey, Phases and phase transitions of the phosphatidylcholines, Biochim. Biophys. Acta 1376 (1998) 91–145.
[31] D. Needham, E. Evans, Structure and mechanical properties of giant lipid (DMPC) vesicle bilayers from 20°C below to 10°C above the liquid crystal–crystalline phase transition at 24°C, Biochemistry 27 (1988) 8261–8269.
[32] E.A. Evans, V.A. Parsegian, Thermal–mechanical fluctuations enhance repulsion between biomolecular layers, Proc. Natl. Acad. Sci. USA 83 (1986) 7132–7136.
[33] W. Helfrich, Elastic properties of lipid bilayers: theory and possible experiments, Z. Naturforsch. 28c (1973) 693–703.
[34] R. Podgornik, V.A. Parsegian, On a possible microscopic mechanism underlying the vapor pressure paradox, Biophys. J. 72 (1997) 942–952.
[35] J. Katsaras, Adsorbed to a rigid substrate, dimyristoylphosphatidylcholine multibilayers attain full hydration in all mesophases, Biophys. J. 75 (1998) 2157–2162.
[36] S. Tristram-Nagle, H.I. Petrache, R.M. Suter, J.F. Nagle, Effect of substrate roughness on D spacing supports theoretical resolution of vapor pressure paradox, Biophys. J. 74 (1998) 1421–1427.
[37] W.J. Sun, S. Tristram-Nagle, R.M. Suter, J.F. Nagle, Structure of gel phase saturated lecithin bilayers – temperature and chain-length dependence, Biophys. J. 71 (1996) 885–891.
[38] S. Kirchner, G. Cevc, Temperature-variation of lipid-membrane structure and the hydration force in fluid lamellar phase – experimental studies with dimyristoylphosphatidylcholine multibilayers, Europhys. Lett. 23 (1993) 229–235.
[39] M.C. Wiener, S.H. White, Structure of a fluid dioleoylphosphatidylcholine bilayer determined by joint refinement of X-ray and neutron-diffraction data. 3. Complete structure, Biophys. J. 61 (1992) 434–447.
[40] H.I. Petrache, N. Gouliaev, S. Tristram-Nagle, R.T. Zhang, R.M. Suter, J.F. Nagle, Interbilayer interactions from high-resolution x-ray scattering, Phys. Rev. E 57 (1998) 7014–7024.
[41] T. Hønger, K. Mortensen, J.H. Ipsen, J. Lemmich, R. Bauer, O.G. Mouritsen, Anomalous swelling of multilammelar lipid bilayers in the transition region by renormalization of curvature elasticity, Phys. Rev. Lett. 72 (1994) 3911–3914.
[42] R. Zhang, W. Sun, S. Tristam-Nagle, R.L. Headrick, R.M. Suter, J.F. Nagle, Critical fluctuations in membranes, Phys. Rev. Lett. 74 (1995) 2832–2835.
[43] J. Lemmich, K. Mortensen, J.H. Ipsen, T. Hønger, R. Bauer, O.G. Mouritsen, Pseudocritical behavior and unbinding of phospholipid bilayers, Phys. Rev. Lett. 75 (1995) 3958–3961.
[44] F.Y. Chen, W.C. Hung, H.W. Huang, Critical swelling of phospholipid bilayers, Phys. Rev. Lett. 79 (1997) 4026–4029.
[45] F. Richter, L. Finegold, G. Rapp, Sterols sense swelling in lipid bilayers, Phys. Rev. E 59 (1999) 3483–3491.
[46] Z. Zhou, B.G. Sayer, R.E. Stark, R.M. Epand, High-resolution magic-angle spinning H-1 nuclear magnetic resonance studies of lipid dispersions using spherical glass ampoules, Chem. Phys. Lipids 90 (1997) 45–53.
[47] L.L. Holte, K. Gawrisch, Determining ethanol distribution in phospholipid multilayers with MAS-NOESY spectra, Biochemistry 36 (1997) 4669–4674.
[48] Z. Zhou, B.G. Sayer, D.W. Hughes, R.E. Stark, R.M. Epand, Studies of phospholipid hydration by high-resolution magic-angle spinning nuclear magnetic resonance, Biophys. J. 76 (1999) 387–399.